

Madurastatin D1 and D2, Oxazoline Containing Siderophores Isolated from an *Actinomadura* sp.

Jia-Xuan Yan,[†] Marc G. Chevrette,^{‡,||} Doug R. Braun,[†] Mary Kay Harper,[§] Cameron R. Currie,^{||} and Tim S. Bugni^{*,†,||}

[†]Pharmaceutical Sciences Division, University of Wisconsin—Madison, 777 Highland Avenue, Madison, Wisconsin 53705, United States

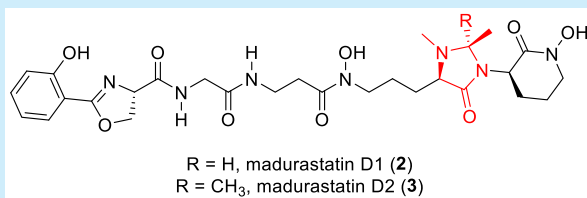
[‡]Department of Genetics, University of Wisconsin—Madison, 425 G Henry Mall, Madison, Wisconsin 53706, United States

[§]Department of Medicinal Chemistry, University of Utah, 30 South 2000 East, Salt Lake City, Utah 84112, United States

^{||}Department of Bacteriology, University of Wisconsin—Madison, 1550 Linden Avenue, Madison, Wisconsin 53706, United States

Supporting Information

ABSTRACT: Two new siderophores, madurastatin D1 and D2, together with (–)-madurastatin C1, the enantiomer of a known compound, were isolated from marine-derived *Actinomadura* sp. The presence of an unusual 4-imidazolidinone ring in madurastatins D1 and D2 inspired us to sequence the *Actinomadura* sp. genome and to identify the *mad* biosynthetic gene cluster, knowledge of which enables us to now propose a biosynthetic pathway. Madurastatin D1 and D2 are moderately active in antimicrobial assays with *M. luteus*.



Siderophores represent a crucial class of bacterial secondary metabolites that are employed as iron chelators by microorganisms to facilitate the absorption of poorly soluble environmental iron.¹ Siderophores feature high binding affinities toward Fe(III) and often contain multiple N, O functionalities.¹ They can also be employed by pathogenic bacteria to acquire iron, the fundamental limiting nutrient for life, from their host organisms and influence the cellular iron level of the hosts.²

The bacterial genus *Actinomadura* from the phylum Actinobacteria has been reported to produce a series of phenolate-hydroxamate siderophores,² including madurastatins^{3–5} and maduraferin.⁶ The madurastatins were first characterized as aziridine-containing pentapeptide siderophores; however, structural revision on the aziridine ring was suggested by Thorson and Shaaban⁷ based on their analyses of siderophores with 2-(2-hydroxyphenyl)oxazoline moieties. NMR data of the isolated madurastatin C1 (also designated as MBJ-0034) from bacteria cell culture and synthetic analogs with aziridine- and 2-(2-hydroxyphenyl)oxazoline moieties were compared by Hall in 2017,⁸ which confirmed the structural revision proposed by Thorson and Shaaban. The absolute configuration of madurastatin C1 (1) (Figure 1) was also established by Hall.⁸

As part of our goal to discover new natural products from marine invertebrate associated bacteria,^{9–11} our attention was drawn to strain WMMA-1423, a marine *Actinomadura* sp. cultivated from the sponge *Tedania* sp., after its crude extract was found to inhibit the growth of both MRSA and *Bacillus subtilis* on agar plates. We isolated two new madurastatins,

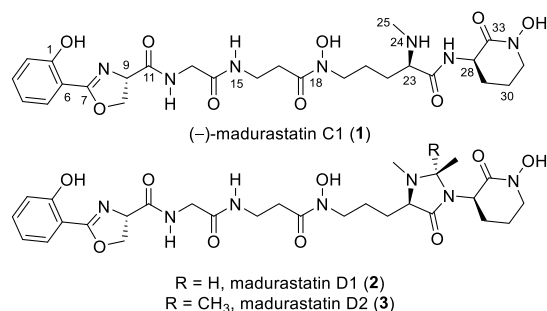


Figure 1. Structures of madurastatin C1 (1), D1 (2) and D2 (3).

madurastatin D1 (2) and D2 (3) (Figure 1), and the enantiomer [1, (–)-madurastatin C1] of the known compound madurastatin C1 by bioassay guided isolation using MRSA (ATCC #33591) as the test strain. Though only slightly active against MRSA (*vide infra*), fractions containing 1–3 were sufficiently active in agar plate assays as to pique our interest. Madurastatin D1 (2) and D2 (3) feature the cyclic 4-imidazolidinone in contrast to the linear α -amino amide in madurastatin C1. Both 2 and 3 exhibited lower MICs against *M. luteus* than 1, suggesting that the additional heterocycle increases antibacterial activity. Due to the unusual cyclization bridging two nitrogens, whole genome sequencing of strain WMMA-1423 was conducted and a biosynthetic pathway to madurastatins D1 and D2 was proposed.

Received: June 21, 2019

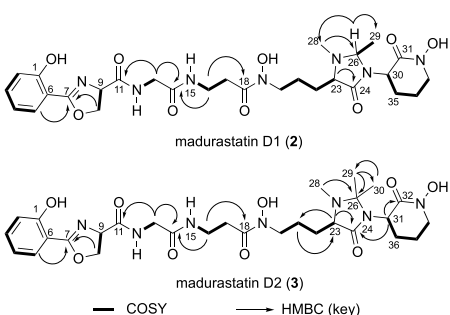
HRMS data suggested the molecular formula of $C_{28}H_{39}N_7O_9$ ($m/z = 618.2876$, $[M + H]^+$) for madurastatin D1 (**2**). Since Fe has a unique isotope distribution (^{54}Fe : ^{56}Fe : $^{57}\text{Fe} \approx 6:92:2$), the observation of Fe(III) adduct ions $[M-2H+Fe]^+$ ($m/z = 671.1991$, Figure S14) was a clear indicator of compound **2**'s ability to bind iron and further confirmation of the assigned molecular ion. Compared to the known madurastatin C1, **2** had one additional degree of unsaturation. By comparing of ^1H and ^{13}C NMR data (Table 1, Figure S3–S7) between the reported madurastatin C1⁸ and **2**, the tertiary carbon C-26 (74.7 ppm) and the methyl group carbon C-29 (19.7 ppm) were observed only in **2**, which have HSQC correlations to H-26 (4.01 ppm) and H-29 (1.21 ppm), respectively. H-26 showed COSY correlations to H-29, and it also showed HMBC correlations to C-28 (37.9 ppm, N-Me group attached to N-25) and to C-29, which suggested the connection between N-25 and C-26. In light of these data, the structure of **2** was assigned as containing the 1, 2-dimethyl-4-imidazolidinone cyclic structure.

A molecular formula of $C_{29}H_{41}N_7O_9$ ($m/z = 632.3025$, $[M + H]^+$) was suggested by HRMS data for madurastatin D2 (**3**). Fe(III) adduct ions $[M+Fe+Na-3H]^+$ ($m/z = 707.1941$) were also observed (Figure S15). The NMR data (Table 1, Figures S8–S12) of **3** was compared to **2** and, since these two compounds have the same number of degrees of unsaturation, a similar 4-imidazolidinone cyclic structure was also proposed for **3** despite a few differences. The major difference was that the tertiary C-26 carbon in **2** was replaced by a tetrasubstituted C-26 (77.9 ppm) in **3**. Two methyl groups (C-29 and C-30) showed HMBC correlations to C-26 and to each other as well, suggesting shared connectivity to the C-26. These two methyl groups also showed different ^{13}C chemical shifts (25.7 ppm for C-29, 19.8 ppm for C-30) and ^1H chemical shifts (1.29 for H-29, 1.11 for H-30), which suggested both of them are connected to a carbon that belongs to a cyclic system. Thus, the structure of **3** was proposed with a similar 1, 2, 2-trimethyl-4-imidazolidinone cyclic structure. Interestingly, the difference in methylation status at C-26 was found to induce slight, but noticeable, differences in the ^{13}C shifts for the N-hydroxy lactams of compounds **2** and **3** as well as a ~ 5 ppm difference in the ^{13}C shifts observed at C-28; these are likely attributable to conformational restrictions encountered by **3** but not **2**.

The siderophoric properties of compounds **1–3** were assessed on the basis of the chrome azurol S (CAS) assay (Figure S16).⁹ Deferoxamine mesylate was also analyzed and served as a positive Fe(III) binding control. The colorimetric CAS assay revealed that **1** and **2** bind iron with efficiencies comparable to deferoxamine mesylate whereas compound **3**, bearing the geminal-dimethyl moiety also bound iron but with noticeably impaired affinity relative to **1** and **2**. This trend in iron binding supports the notion that C-26 dimethylation imparts conformational limitations to **3** that are lacking in compounds **1** and **2**.

The absolute configuration of madurastatin C1 was determined by Hall and co-workers⁸ using the Marfey's method (Figure S17).¹² The ^{13}C chemical shifts (Figure S2) of **1** were identical to those reported for madurastatin C1 although the optical rotation of **1** was found to be inverted from that of madurastatin C1. The C-9 configuration of madurastatin C1 was shown to be 9R by Marfey's method.^{8,12} Thus, we determined that **1** is the enantiomer of madurastatin C1 and has stereocenter assignments as 9S, 23R, 28R. Notably, enantiomeric natural product pairings are well-known and have

Table 1. ^1H and ^{13}C NMR Data for **2** and **3** (600 MHz for ^1H , 125 MHz for ^{13}C , d_6 -DMSO)



position	2		3	
	δ_C , type	δ_H (J in Hz)	δ_C , type	δ_H (J in Hz)
1	159.1		159.1	
2	116.7, CH	7.01, d (8.4)	116.7, CH	6.98, d (7.6)
3	134.1, CH	7.47, ddd (8.4, 7.3, 1.6)	134.1, CH	7.45, t (7.6)
4	119.1, CH	6.95, t (7.5)	119.0, CH	6.91, t (7.6)
5	128.1, CH	7.64, dd (7.6, 1.4)	128.1, CH	7.63, d (7.4)
6	110.0		110.0	
7	165.9		165.9	
9	67.5, CH	5.01, dd (10.4, 7.7)	67.4, CH	5.00, dd (10.2, 8.0)
10	69.5, CH ₂	4.65, dd (10.3, 8.5)	69.4, CH ₂	4.63, dd (10.2, 8.1)
		4.51, t (8.0)		4.51, t (8.3)
11	170.2		170.2	
12		8.61, t (5.9)		8.56, s
13	42.2, CH ₂	3.73, dd (16.6, 6.0)	42.2, CH ₂	3.75, d (16.0)
		3.67, dd (16.6, 6.0)		3.66, d (16.0)
14	168.4		168.4	
15		8.01, t (5.4)		7.97, s
16	34.7, CH ₂	3.24, dd (6.6, 6.0)	34.8, CH ₂	3.25, dd (7.0, 5.6)
17	31.9, CH ₂	2.56–2.48, m	31.7, CH ₂	2.50–2.55, m
18	170.8		170.6	
20	47.4, CH ₂	3.51–3.42, m	51.1, CH ₂	3.41–3.53, m
21	21.6, CH ₂	1.70–1.43, m	20.9, CH ₂	1.36–1.46, m
22	26.6, CH ₂	1.53–1.43, m	25.0, CH ₂	1.85–1.94, m
		1.98–1.82, m		
23	64.8, CH	2.88, m	62.0, CH	2.93, t (5.0)
24	171.6		169.9	
26	74.7, CH	4.01, q (5.0)	77.9	
28	37.9, CH ₃	2.29, s	32.5, CH ₃	2.24, s
29	19.7, CH ₃	1.21, d (5.2)	25.7, CH ₃	1.29, s
30	51.8, CH	4.32–4.24, m	19.8, CH ₃	1.11, s
31	162.4		51.7, CH	3.91, dd (6.0, 5.4)
32			163.3	
33	51.1, CH ₂	3.51–3.57, m		
		3.41–3.46, m		
34	21.6, CH ₂	1.87–1.79, m	47.5, CH ₂	3.43–3.47, m
35	21.3, CH ₂	2.03–1.95, m	21.3, CH ₂	1.67–1.73, m
				1.84–1.93, m
36			25.5, CH ₂	2.34–2.42, m
				1.67–1.73, m

been rigorously reviewed.¹³ Since **2** and **3** were produced by the same organism, both compounds were proposed to have

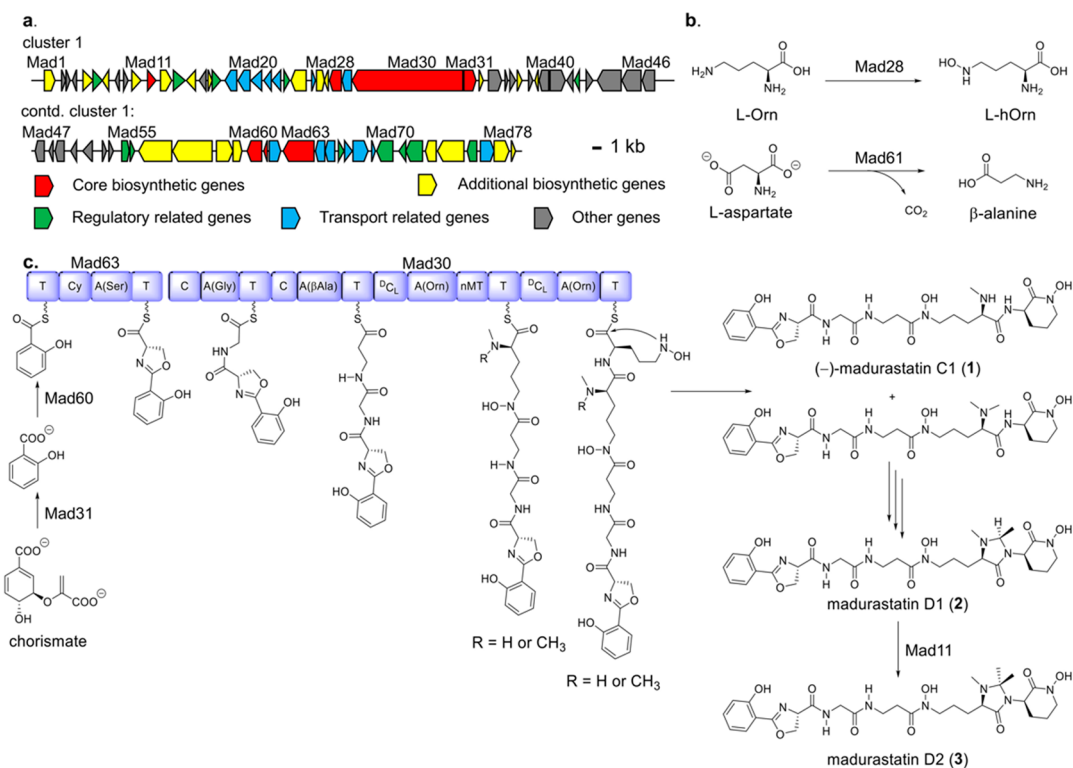


Figure 2. (a) Organization of *mad* cluster. (b) Proposed functions of Mad28 and Mad61 as building block producers, and (c), Proposed biosynthetic pathway to 1–3. Domain annotations: A, adenylation; C, condensation; Cy, cyclization; ^DC_L, epimerization/condensation; T, thiolation; nMT, N-methylation.

the same configuration as found in **1** [9S, 23R, 30R (31R for **3**)]. Further efforts to determine the configuration of C-26 in **2** employed molecular modeling and density functional theory (DFT) NMR calculations of the two models (23R, 26R, 30R- and 23R, 26S, 30R-). Spartan 14 (v.1.1.7 Wave function Inc. 2014) was used to identify the conformer Boltzmann distribution for each diastereoisomer using molecular mechanics. Gaussian 09 was then used to optimize the local geometry of the low energy conformers based on DFT energy calculation (B3LYP/6-31G(d,p)), and the NMR chemical shifts of different stereoisomers were calculated using GIAO method (Table S1). NMR chemical shifts were referenced to TMS and benzene using the multistandard method.¹⁴ The DP4 probability method¹⁵ was used to compare the calculated ¹³C NMR chemical shifts of the two models with the experimental ¹³C chemical shifts and yielded a 100% probability for the *R* compared to the *S* configuration (Table S2).

Previous reports have shown that madurastatin C1 inhibits the growth of *M. luteus*.⁴ Therefore, compounds 1–3 were tested for antibacterial activity against *M. luteus*. Notably, compounds 2 and 3 both inhibited *M. luteus* with MICs of 25.3 and 25.8 μM , respectively; the MIC of compound 1, devoid of the imidazolidinone, was 108.1 μM . Thus, the 4-imidazolidinone clearly benefits the antibacterial activity of these agents although efforts to elucidate the specific mechanisms at play are beyond the scope of this report. Noteworthy is that, although MRSA proved important during bioassay-guided fractionation, none of the new madurastatins inhibited MRSA with MICs less than 100 μM .

To identify the biosynthetic cluster for madurastatin D1 (1) biosynthesis, the whole genome of *Actinomadura* sp. WMMA-

1423 was sequenced (GenBank accession number CP041244) and analyzed using antiSMASH (version 5.0.0 rc1).^{16,17} Two gene clusters (57.9 kb and 46.7 kb, respectively) were identified as the nonribosomal peptide synthetases (NRPSs), transport and regulatory genes for (–)-madurastatin C1 (1), madurastatin D1 (2) and madurastatin D2 (3) production. Although antiSMASH identified these as separate clusters, they were found to be colocalized in the genome (12.1 kb apart from each other) and thus, represent one cluster. The architecture and annotation of the madurastatin (*mad*) biosynthetic gene cluster are shown in [Figure 2](#) and [Table S3](#). The *mad* cluster consists of two NRPS genes ([Figure 2a](#), red, *mad30*, *mad63*), two chain initiation genes (red, *mad31*, *mad60*), two amino acid tailoring genes (red, *mad28*, *mad61*), one S-adenosyl-methionine (SAM)-dependent methyltransferase gene (red, *mad11*) as well as additional biosynthetic (yellow), transport (teal), regulation-related (green) and other genes (gray); full annotations are provided in [Table S3](#)). Most of the proteins encoded in the *mad* cluster are homologous to those involved in cahuitamycin,¹⁸ albachelin,¹⁹ and amyachelin²⁰ biosynthetic pathways. The genome analysis has allowed us to put forth a hypothesis with regard to the possible biosynthesis of madurastatins, where a SAM-dependent mechanism is involved in the biosynthesis of madurastatin D2 ([Figure 2c](#), [Table S3](#)). Further biosynthetic studies to more completely understand the assembly of 1–3, with special emphasis on the unique imidazolidinone of 2 and 3, are clearly warranted.

Mad28, Mad61 are likely ornithine N-monooxygenase and aspartate 1-decarboxylase enzymes, responsible for generating the L-N-OH-Orn (L-hOrn) and β -alanine moieties, respectively.

Mad31 is homologous to salicylate synthase AmcL in amycolin biosynthesis (59% identity) and Mad60 is homologous to the salicylate-AMP ligase CahJ (67% identity) in cahuitamycin biosynthesis. Together, Mad31 and Mad60 likely catalyze the formation of a Mad63-salicylate conjugate starting from chorismate. Mad63 contains one set of C, A, T domains and very likely installs the oxazoline ring since it shows 58% identity to CahA; CahA contains a cyclization domain that creates the oxazoline ring in cahuitamycins. We envision that the growing chain is further extended by Mad30, which contains four sets of C, A, T domains and one N-methylation (nMT) domain; antiSMASH analysis revealed that two of the C domains function as ^DC_L domains (Figure 2c). The A domains in Mad30 are proposed to activate Gly, β-Ala and L-hOrn substrates. We envision that epimerization of each L-hOrn, accounting ultimately for the R stereocenters found in 1–3, likely results from the dual epimerase/condensation activities of the ^DC_L domains.²¹

The nMT domain located between the third and fourth A domains is envisioned to catalyze both mono- and dimethylation of the α-amine group of the initially added D-hOrn. Both mono- and dimethylated intermediates would undergo further condensation to add on the final hOrn unit. Intramolecular nucleophilic substitution is then proposed to install the N-hydroxy lactam (with liberation from Mad30) to afford (–)-madurastatin C1 (1) and the dimethylated variant of 1; both are possible intermediates en route to madurastatin D1 (2) although we favor the dimethylated species based on its complete absence during the course of compound isolations. We envision that N-Me oxidation may play a central role in imidazolidinone assembly, from the dimethylated version of 1, although it is not yet clear which gene/s in the *mad* cluster would code for this chemistry (Figure 2c). In proceeding from 2 to 3, we invoke the SAM-dependent methyltransferase Mad11; SAM-dependent methylation at both sp² and sp³ carbons adjacent to heteroatoms are well-known.^{22–25} At present, Mad11 appears to be the most likely candidate for converting monomethylated 2 into dimethylated madurastatin D2 (3).

In summary, we report the isolation and structural elucidation of madurastatin D1 (2) and D2 (3), two new madurastatin siderophores that showed *in vitro* activity against *M. luteus*. To the best of our knowledge, only five other madurastatin analogs^{3–5} have been isolated from *Actinomadura* sp., and none of them contain the 4-imidazolidinone cyclic moiety. The biosynthetic origins for this unique structure are currently unclear although we hypothesize that a combination of methyltransferase and oxidase chemistries may prove central. While scientifically intriguing, further studies will be required to test this biosynthetic hypothesis.

■ ASSOCIATED CONTENT

● Supporting Information

The Supporting Information is available free of charge on the ACS Publications website at DOI: 10.1021/acs.orglett.9b02159.

Procedures and NMR, gCOSY, and gHSQC spectra (PDF)

■ AUTHOR INFORMATION

Corresponding Author

*E-mail: tim.bugni@wisc.edu.

ORCID

Tim S. Bugni: 0000-0002-4502-3084

Notes

The authors declare no competing financial interest.

■ ACKNOWLEDGMENTS

This work was supported by funding from the University of Wisconsin-Madison School of Pharmacy and the Graduate School at the University of Wisconsin. This work was also funded by the NIH Grant U19AI109673 and U19AI142720. We would like to thank the Analytical Instrumentation Center at the School of Pharmacy, University of Wisconsin-Madison for the facilities to acquire spectroscopic data. This study made use of the National Magnetic Resonance Facility at Madison, which is supported by NIH grant P41GM103399 (NIGMS). Additional equipment was purchased with funds from the University of Wisconsin, the NIH (RR02781, RR08438), the NSF (DMB-8415048, OIA-9977486, BIR-9214394), and the USDA.

■ REFERENCES

- (1) Hider, R. C.; Kong, X. *Nat. Prod. Rep.* **2010**, *27*, 637–657.
- (2) Miethke, M.; Marahiel, M. A. *Microbiol. Mol. Biol. Rev.* **2007**, *71*, 413–451.
- (3) Harada, K.; Tomita, K.; Fujii, K.; Masuda, K.; Mikami, Y.; Yazawa, K.; Komaki, H. *J. Antibiot.* **2004**, *57*, 125–135.
- (4) Mazzei, E.; Iorio, M.; Maffioli, S. I.; Sosio, M.; Donadio, S. *J. Antibiot.* **2012**, *65*, 267–269.
- (5) Kawahara, T.; Itoh, M.; Izumikawa, M.; Sakata, N.; Tsuchida, T.; Shin-ya, K. *J. Antibiot.* **2014**, *67*, 577–580.
- (6) Keller-Schierlein, W.; Hagmann, L.; Zähler, H.; Huhn, W. *Helv. Chim. Acta* **1988**, *71*, 1528–1540.
- (7) Shaaban, K. A.; Saunders, M. A.; Zhang, Y.; Tran, T.; Elshahawi, S. I.; Ponomareva, L. V.; Wang, X.; Zhang, J.; Copley, G. C.; Sunkara, M.; Kharel, M. K.; Morris, A. J.; Hower, J. C.; Tremblay, M. S.; Prendergast, M. A.; Thorson, J. S. *J. Nat. Prod.* **2017**, *80*, 2–11.
- (8) Tyler, A. R.; Mosaei, H.; Morton, S.; Waddell, P. G.; Wills, C.; McFarlane, W.; Gray, J.; Goodfellow, M.; Errington, J.; Allenby, N.; Zenkin, N.; Hall, M. *J. Nat. Prod.* **2017**, *80*, 1558–1562.
- (9) Zhang, F.; Barns, K.; Hoffmann, F. M.; Braun, D. R.; Andes, D. R.; Bugni, T. S. *J. Nat. Prod.* **2017**, *80*, 2551–2555.
- (10) Wyche, T. P.; Standiford, M.; Hou, Y.; Braun, D.; Johnson, D. A.; Johnson, J. A.; Bugni, T. S. *Mar. Drugs* **2013**, *11*, 5089–5099.
- (11) Wyche, T. P.; Piotrowski, J. S.; Hou, Y.; Braun, D.; Deshpande, R.; McIlwain, S.; Ong, I. M.; Myers, C. L.; Guzei, I. A.; Westler, W. M.; Andes, D. R.; Bugni, T. S. *Angew. Chem., Int. Ed.* **2014**, *53*, 11583–11586.
- (12) Marfey, P. *Carlsberg Res. Commun.* **1984**, *49*, 591–596.
- (13) Finefield, J. M.; Sherman, D. H.; Kreitman, M.; Williams, R. M. *Angew. Chem., Int. Ed.* **2012**, *51*, 4802–4836.
- (14) Sarotti, A. M.; Pellegrinet, S. C. *J. Org. Chem.* **2009**, *74*, 7254–7260.
- (15) Smith, S. G.; Goodman, J. M. *J. Am. Chem. Soc.* **2010**, *132*, 12946–12959.
- (16) Blin, K.; Shaw, S.; Steinke, K.; Villebro, R.; Ziemert, N.; Lee, S. Y.; Medema, M. H.; Weber, T. *Nucleic Acids Res.* **2019**, *47*, W81–W87.
- (17) Blin, K.; Wolf, T.; Chevrete, M. G.; Lu, X.; Schwalen, C. J.; Kautsar, S. A.; Duran, H. G. S.; de los Santos, E. L. C.; Kim, H. U.; Nave, M.; Dickschat, J. S.; Mitchell, D. A.; Shelest, E.; Breitling, R.; Takano, E.; Lee, S. Y.; Weber, T.; Medema, M. H. *Nucleic Acids Res.* **2017**, *45*, W36–W41.
- (18) Park, S. R.; Tripathi, A.; Wu, J.; Schultz, P. J.; Yim, I.; McQuade, T. J.; Yu, F.; Arevang, C. – J.; Mensah, A. Y.; Tamayo-Castillo, G.; Xi, C.; Sherman, D. H. *Nat. Commun.* **2016**, *7*, 10710.

- (19) Kodani, S.; Komaki, H.; Suzuki, M.; Hemmi, H.; Ohnishi-Kameyama, M. *BioMetals* **2015**, 28, 381–389.
- (20) Seyedsayamdost, M. R.; Traxler, M. F.; Zheng, S. – L.; Kolter, R.; Clardy, J. *J. Am. Chem. Soc.* **2011**, 133, 11434–11437.
- (21) Rausch, C.; Hoof, I.; Weber, T.; Wohlleben, W.; Huson, D. H. *BMC Evol. Biol.* **2007**, 7, 78.
- (22) Grove, T. L.; Benner, J. S.; Radle, M. I.; Ahlum, J. H.; Landgraf, B. J.; Krebs, C.; Booker, S. J. *Science* **2011**, 332, 604–607.
- (23) Buckel, W.; Thauer, R. K. *Angew. Chem., Int. Ed.* **2011**, 50, 10492–10494.
- (24) Kim, H. J.; McCarty, R. M.; Ogasawara, Y.; Liu, Y. – N.; Mansoorabadi, S. O.; LeVieux, J.; Liu, H. – W. *J. Am. Chem. Soc.* **2013**, 135, 8093–8096.
- (25) Woodyer, R. D.; Li, G.; Zhao, H.; van der Donk, W. A. *Chem. Commun.* **2007**, 28, 359–361.